



BRILL

## TRACHEID AND PIT ANATOMY VARY IN TANDEM IN A TALL *SEQUOIADENDRON GIGANTEUM* TREE

Martina Lazzarin<sup>1</sup>, Alan Crivellaro<sup>1</sup>, Cameron B. Williams<sup>2</sup>, Todd E. Dawson<sup>2</sup>,  
Giacomo Mozzi<sup>1</sup>, and Tommaso Anfodillo<sup>1,\*</sup>

<sup>1</sup>Dipartimento Territorio e Sistemi Agro Forestali, Università degli Studi di Padova,  
35020 Legnaro (PD), Italy

<sup>2</sup>Department of Integrative Biology, University of California, Berkeley, California 94720, U.S.A.

\*Corresponding author; e-mail: tommaso.anfodillo@unipd.it

### ABSTRACT

Across land plants there is a general pattern of xylem conduit diameters widening towards the stem base thus reducing the accumulation of hydraulic resistance as plants grow taller.

In conifers, xylem conduits consist of cells with closed end-walls and water must flow through bordered pits imbedded in the side walls. As a consequence both cell size, which determines the numbers of walls that the conductive stream of water must cross, as well as the characteristics of the pits themselves, crucially affect total hydraulic resistance. Because both conduit size and pit features influence hydraulic resistance in tandem, we hypothesized that features of both should vary predictably with one another. To test this prediction we sampled a single tall (94.8 m) *Sequoiadendron giganteum* tree (giant sequoia), collecting wood samples from the most recent annual ring progressively downwards from the tree top to the base. We measured tracheid diameter and length, number of pits per tracheid, and the areas of pit apertures, tori, and margos. Tracheid diameter widened from treetop to base following a power law with an exponent (tracheid diameter-stem length slope) of approximately 0.20. A similar scaling exponent was found between tracheid length and distance from tree top. Additionally, pit aperture, torus, and margo areas all increased (again with a power of ~0.20) with distance from tree top, paralleling the observed variation in tracheid diameter and length. Pit density scaled isometrically with tracheid length. Within individual tracheids, total permeable area of pits, measured as the sum of the margo areas, scaled isometrically with lumen area. Given that pores of the margo membrane are believed to increase in parallel with membrane area, from a strictly anatomical perspective, our results support the interpretation that pit resistance remains a relatively constant fraction of total resistance along the hydraulic pathway.

**Keywords:** Allometric scaling, margo, hydraulic resistance.

## INTRODUCTION

The study of very tall trees (*i.e.* >90 m in height) provides a unique opportunity to assess how axial variation in the structure of the water transport system can maintain an efficient water supply to the leaves. The diameter of the xylem conduits and the size and density of the side-wall pits are two main components governing the hydraulic efficiency within the xylem.

Since early anatomical investigations, it has been known that tracheid size varies along the stem (Sanio 1872), and recent models predict the optimal rate of tracheid diameter increase from the tip to the stem base (West *et al.* 1999). The hydraulic resistance through a cylindrical pipe increases linearly to its length but it is inversely related to the 4<sup>th</sup> power of its diameter. A slight increase in diameter thus will produce a disproportionate decrease in hydraulic resistance (Becker *et al.* 2003). The same principle applies to trees, in the pipelines along the main stem axis. In fact, the diameter of tracheids within the same growth ring widen toward the base of the tree (Anfodillo *et al.* 2013). Consequently the accumulation of hydraulic resistance is buffered from added path length (*i.e.*, tree height), and it has even been proposed that resistance may become independent of path length if basipetal conduit widening is sufficient (West *et al.* 1999).

Variation in xylem conduit diameter along the stem has been extensively studied, and the rate of conduit widening (*i.e.* the exponent of the conduit diameter-stem length/distance from the stem tip power function) towards the stem base is remarkably similar among plants of different sizes, species, and environments (Leicht 2001; Weitz *et al.* 2006; Anfodillo *et al.* 2006; Coomes *et al.* 2007; Petit *et al.* 2008, 2009, 2010; Olson *et al.* 2014).

The role of tracheid length in determining the total resistance is less straightforward. It has been proposed (Comstock & Sperry 2000) that increasing the length of a single tracheid reduces the total number of tracheids needed to build the entire pipeline, thus reducing the number of tracheid-to-tracheid transfers through the pits and the resistance along the entire pathway. However, the resistance of a conduit lumen decreases disproportionately with an increase in lumen diameter, but the resistance of the inter-conduit pit resistance decreases linearly. As a result the contribution of the pits to total resistance might be predicted to become progressively more limiting with increasing tracheid length. But this functional constraint occurs only if the pit resistance (*i.e.* margo permeability) does not change with tracheid length. Recent findings, however, show the contrary; that is, that pit conductance markedly increases with tracheid size (Schulte *et al.* 2015). Thus, the simple cascade of events relating tracheid length and total pit resistance proposed by Comstock and Sperry (2000) might be reconsidered by analyzing how pit structure and density vary with tracheid length or diameter.

Pits are holes in the secondary cell walls of xylem conduits. They are made up of an aperture, the narrow end of the hole and the one that gives onto the conduit interior. The aperture widens like a short, broad funnel into the pit chamber, which meets an identical aperture with mirror image that enters the chamber from the adjacent conduit cell. The primary walls and intervening middle lamellae of two opposing cells make up the pit membrane, which lies in the centre of the pit pair (Choat *et al.* 2008; Li *et al.*

2016). In most conifers the pit membrane has two distinct regions. The central region consists of a lenticular thickening, called the torus, which is considered impermeable, while the outer region of the membrane, the margo, is porous and permeable to xylem sap. Pit resistance occurs when sap flows between adjacent tracheids, and the total hydraulic resistance is strongly influenced by the size of pores in the membrane, pit aperture size and pit density within the cell wall (Schulte *et al.* 2015). All these features also greatly affect cavitation resistance of connected tracheids (Jansen *et al.* 2011).

Previous studies partitioned the total hydraulic resistance into pit and lumen resistances. According to Sperry *et al.* (2006), a constant 64% of the total hydraulic resistance is contributed by the pits, while the remainder is contributed by tracheid lumina. Other research shows pit membrane resistance accounts for 14–59% of total resistance (Schulte & Gibson 1988). Becker *et al.* (2003) argues instead that as tracheid lumen diameter increases, the proportion of total resistance attributed to the lumen decreases, while pit membrane resistance increases. Thus, conduit diameter and length, in combination with the number and structure of pits, should influence the ability of water to flow through the hydraulic pathway from tree base to tree top.

Although several studies have measured pit anatomical properties in branches along within-tree height gradients (*e.g.*, Burgess *et al.* 2006), few have explored anatomical variation of pits along the main axis of the hydraulic pipeline (*i.e.*, trunk). However, Bailey and Faull (1934) did compare intertracheid pits of rootwood, trunkwood and branchwood of another giant taxodioid conifer, *Sequoia sempervirens* and found that pit diameter and frequency scales with tracheid size and diameter. Domec *et al.* (2006) found that a reduction in whole-wood specific conductivity was due to a decrease in pit aperture as well as the size and number of margo pores higher in the trunks of *Pseudotsuga menziesii* (Douglas-fir) trees. Also in Douglas-fir, Domec *et al.* (2008) showed that the ratio of torus diameter/pit aperture diameter increased towards the tree top, suggesting higher resistance to cavitation at the expense of reducing hydraulic conductivity. However, these studies did not consider concomitant changes in tracheid and pit dimensions with plant height in the context of minimizing total axial hydraulic resistance. The stable and universal hydraulic design of pipeline widening basipetally along the main stem axis (Anfodillo *et al.* 2006; Olson *et al.* 2014) suggests that these anatomical traits might change accordingly.

Our study quantifies axial variation in tracheid size, including diameter and length, as well as pit density and structure, including number of pits per tracheid and the areas of pit apertures, tori, and margos, along the main stem axis of a single tall *Sequoiadendron giganteum* (Lindl.) J. Buchh., “Giant Sequoia”. We hypothesized that these anatomical features would change in concert along the main stem axis, thus supporting the notion that pit resistance is a constant proportion of the total tracheid resistance within an optimized hydraulic pathway.

## MATERIALS AND METHODS

### *Site and species*

We selected a single giant sequoia tree based on height, accessibility, and a healthy appearance. The tree was 94.8 m tall, 3.66 m DBH, approximately 3000 years old

(Sillett *et al.* 2015). It is growing adjacent to an alluvial floodplain in an old-growth giant sequoia stand in Kings Canyon National Park, California (36.56° N, 118.77° W). Using tree-climbing equipment to access the entire length of the main stem axis, we collected cores and apical stem portions. Positions of cores and samples along the stem axis are described in Table 1.

Table 1. Location of the collected samples along the stem axis in *Sequoiadendron giganteum* (tree height 94.8 m).

Sample height from the ground (m)	Distance from the tree top (m)
94.785	0.015
94.730	0.070
92.300	2.500
90.000	4.800
85.000	9.800
80.000	14.800
75.000	19.800
70.000	24.800
60.000	34.800
50.000	44.800
40.000	54.800
30.000	64.800
20.000	74.800
10.000	84.800

### *Anatomical features*

We made transverse and tangential sections (15–25 µm thick) from rehydrated core parts (1–2 cm long) containing a few outermost growth rings by using disposable blades on a rotary microtome. The sections were stained with astra blue and safranin, dehydrated with ethanol and xylene, and mounted in Canada balsam (Gärtner & Schweingruber 2013). The tori stained blue, while the tracheid cell walls richer in lignin stained red. Images of the cross- and tangential sections were taken using a digital camera mounted to a Nikon Eclipse 80i compound light microscope. To quantify cross-sectional lumen area, we defined a zone of the outer complete growth ring between two rays and that was large enough to contain at least 100 tracheids. For this zone, we estimated the lumen area of all tracheids, and then converted these areas to lumen diameters ( $d$ ), assuming tracheids were square in cross section using  $d = A^{1/2}$  where  $A$  is the cross-sectional lumen area. Hydraulic diameter ( $D_h$ ) was calculated as  $D_h = (\sum d^5/n)^{1/4}$ , where  $d$  is the diameter of each tracheid and  $n$  is the number of conduits measured (Sperry *et al.* 1994).

In addition to the transverse and tangential sections, a few 40-micron-thick radial sections were cut from the earlywood part of the outermost growth ring and then macerated for 2 hours in a solution of hydrogen peroxide, 40% acetic acid, and water in a 1 : 1 : 1 ratio (Gärtner & Schweingruber 2013). Tracheid lengths ( $T_l$ ) and pit number per tracheid were counted in the macerated material. The number of inter-tracheid pits on the radial face of each tracheid was also counted. Due to the small number of intact

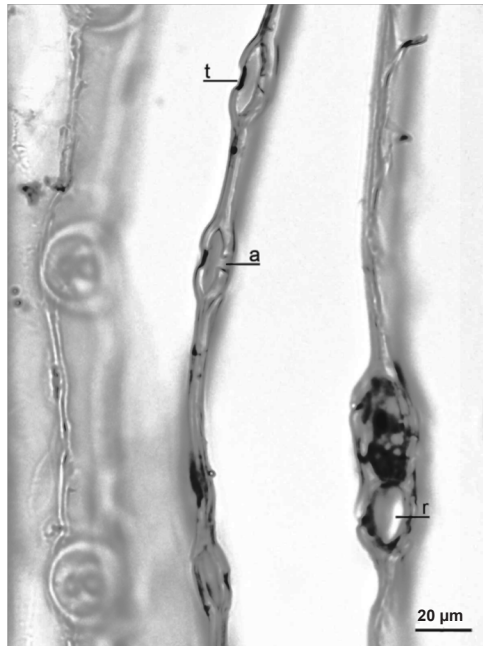


Figure 1. Earlywood tracheids and bordered pits in tangential section of *Sequoiadendron giganteum* (t: torus, a: aperture, r: ray cell).

cells obtained after maceration (due to the long tracheids intersecting with the margins of the cores), the analysis was restricted to five tracheids for eight of our wood samples (levels along the stem). Pit anatomical features were studied in tangential sections cut from the earlywood of the outermost growth ring (magnification of  $500\times$ ) (Fig. 1). For each sample ten pits were analyzed by measuring chamber, torus, and aperture diameters, which were converted to areas by assuming they were circular using  $A = 0.785 d_p^2$  where  $d_p$  is the measured diameter. Margo area was computed by subtracting the area of the torus from the area of the pit chamber, while the total margo area per tracheid was calculated as the product of the margo area per pit and pit number per tracheid. The image-analysis program ImageJ (National Institutes of Health, USA; <http://rsb.info.nih.gov/ij/>) was used to measure the anatomical features.

A significant difference of the slopes was considered when the 95% confidence intervals of the linear regressions did not overlap.

## RESULTS

### *Tracheid diameter and length*

Consistent with our hypothesis, hydraulic diameters ( $D_h$ ) increased basipetally with the distance from the tree top ( $L$ ) following a power trajectory with an estimated exponent of 0.19 (Fig. 2). The absolute variation in  $D_h$  was from  $10\ \mu\text{m}$  1.5 cm below the apical bud to  $46\ \mu\text{m}$  at the stem base. Tracheid length increased basipetally with  $L$

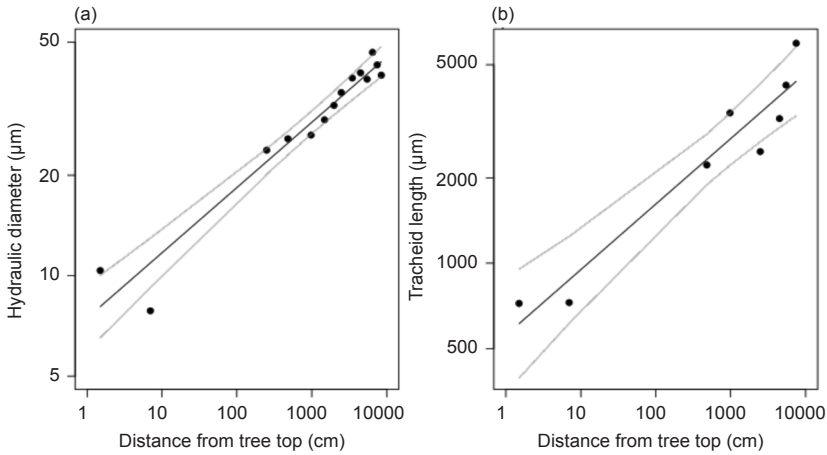


Figure 2. Scaling of (a) hydraulic diameter ( $r^2 = 0.94$ ,  $p < 0.001$ ,  $b = 0.19$ ) and (b) length of tracheids ( $r^2 = 0.92$ ,  $p < 0.001$ ,  $b = 0.23$ ) vs distance from tree top in *Sequoiadendron giganteum*. The axes are shown in log-log scale. 95% confidence intervals are indicated by grey lines.

with an exponent of 0.23, which was not statistically different from  $D_h \propto L^{0.20}$  (Fig. 2). Maximum tracheid length was about 5.6 mm (sample 20 m from the ground).  $T_l$  was found to scale isometrically ( $b = 1.13$ ; 95% CI 0.75–1.51,  $p < 0.001$ ) with  $D_h$  (data not shown) similarly to results reported from Schulte (2012) in three Douglas-fir trees.

### Pit structure

Pit anatomical characteristics in the giant sequoia changed with height and were well correlated with variation in  $D_h$ . In general, pit chamber and torus areas increased towards the stem base according to the variation in  $D_h$ . The scaling exponents were not statistically different from 0.20 for these anatomical traits (Fig. 3). Variation in

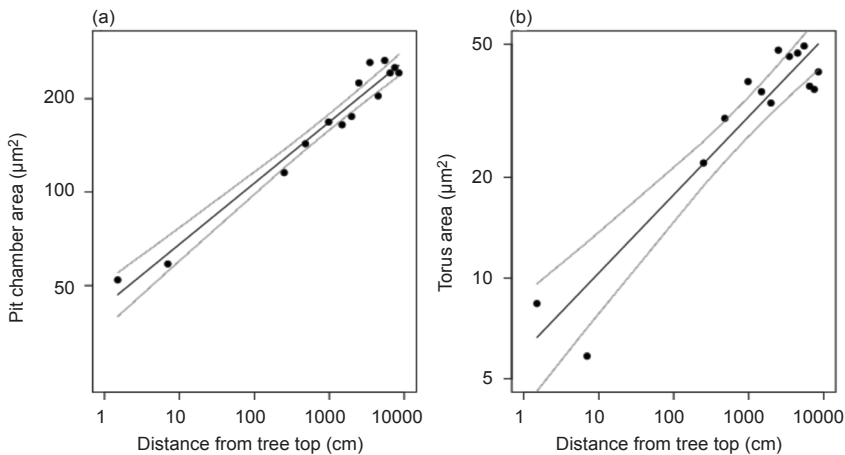


Figure 3. Variation in (a) pit chamber area ( $r^2 = 0.96$ ,  $p < 0.001$ ,  $b = 0.20$ ) and (b) torus area ( $r^2 = 0.88$ ,  $p < 0.001$ ,  $b = 0.23$ ) vs distance from tree top in *Sequoiadendron giganteum*. The axes are shown in log-log scale. 95% confidence intervals are indicated by grey lines.

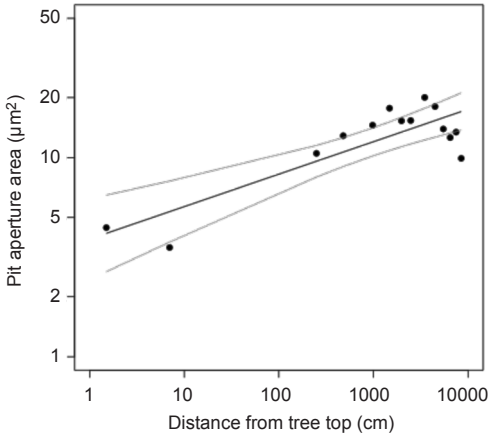


Figure 4. Variation in pit aperture area ( $r^2 = 0.72$ ,  $p < 0.001$ ,  $b = 0.16$ ) vs distance from tree top in *Sequoiadendron giganteum*. The axes are shown in log-log scale. 95% confidence intervals are indicated by grey lines.

pit aperture area had a different pattern, with an increase towards the base until about 50 m from the apex, followed by a decrease to the stem base (Fig. 4). It should be noted that, excluding the lower 4 sampling points (from 54.8 to 84.8 m from the apex), the regression line followed a strict power law ( $b = 0.21$  and  $r^2 = 0.933$ ).

#### *Pit number and permeable area of tracheids*

Pit number scaled isometrically with  $D_h$  (Fig. 5a), so wider and longer tracheids had proportionally more pits. Pit number varied from 53 at 1.5 cm from the tree top, to 243 at 74.8 m from the tree top. As a consequence of the isometric scaling of tracheid diameter vs  $T_l$ , pit number also increased linearly with tracheid length (Fig. 5b; exponent  $b$  not different from 1). Importantly, at a given axial position along the stem, the permeable area of the pits scaled linearly with tracheid area (Fig. 6).

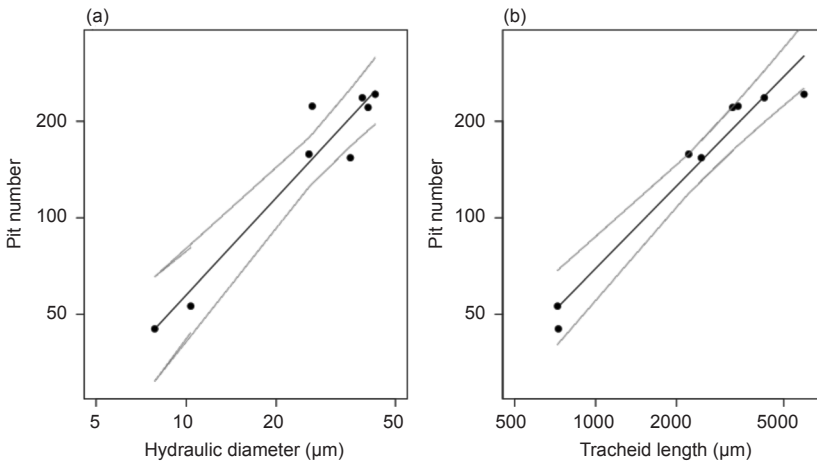


Figure 5. Variation in (a) pit number ( $r^2 = 0.92$ ,  $p < 0.001$ ,  $b = 1.01$ , 95% CI 0.72–1.30) vs hydraulic tracheid diameter and (b) tracheid length ( $r^2 = 0.95$ ,  $p < 0.001$ ,  $b = 0.86$ , 95% CI 0.66–1.05) in *Sequoiadendron giganteum*. The axes are shown in log-log scale.

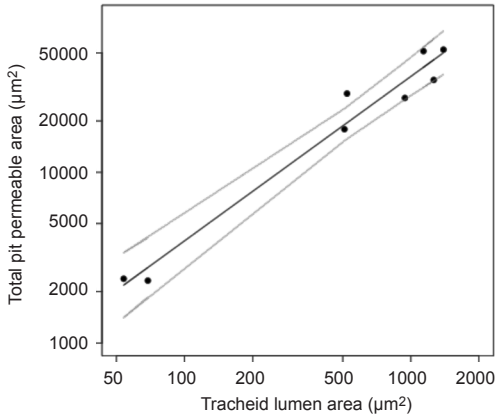


Figure 6. Variation in total pit permeable area (sum of margo areas) vs tracheid lumen area ( $r^2 = 0.97$ ,  $p < 0.001$ ,  $b = 0.96$ ) in *Sequoiadendron giganteum*. The axes are shown in log-log scale. 95% confidence intervals are indicated by grey lines.

## DISCUSSION

### *Tracheid dimensions*

Conduit dimensions and pit structure affect the total transport efficiency of the hydraulic pathway. Our results support the model that basipetal conduit widening acts in a manner to reduce the accumulation of hydraulic resistance with added path length as trees grow taller. Conduit diameters ( $D_h$ ) increased basipetally at a rate consistent with theoretical predictions (Fig. 2), and within the range of those reported in the literature for conifers (scaling exponent of 0.20–0.24) (Anfodillo *et al.* 2006; Weitz *et al.* 2006; Coomes *et al.* 2007; Mencuccini *et al.* 2007; Petit *et al.* 2008, 2009, 2010, 2011). The slightly smaller exponent (*i.e.* 0.19) in this giant sequoia could suggest that this individual might be very close to its maximum height and no longer capable of adjusting (*i.e.* widening) the cell size to completely compensate for further height growth. Indeed, a flatter exponent (*e.g.* 0.15) of the scaling relationship between  $D_h$  vs  $L$  would mean that, as the tree grows taller, the total hydraulic resistance increases which would lead to a progressive decrease of height growth due to the associated deeper water deficit of the tree top leaves.

We found tracheid length ( $T_l$ ) to scale isometrically with tracheid diameter in accordance with data reported from Douglas-fir (Schulte 2012) and with Pittermann *et al.* (2006) who found a nearly isometric relationship from a wide taxonomic sampling of conifer stems and roots (see Data Supplement SI in Pittermann *et al.* 2006). However, Hacke and Jansen (2009) reported a smaller scaling exponent of 0.77 for the inverse relationship between tracheid diameter vs  $T_l$  in *Abies balsamea*, *Picea glauca*, and *Picea mariana* (this means that  $T_l$  scales with tracheid diameter with exponent of 1.2).

The isometric (or larger than 1) scaling between  $T_l$  and  $D_h$  could be explained by the tracheid shape and packing that form the xylem. In contrast, a self-supporting structure such as a column follows the buckling “rule”, where the height vs diameter relationship exhibits a scaling exponent close to 2/3 (McMahon & Kronauer 1976), which means that for supporting taller columns a more than proportional increase in stem diameter is needed. The isometric relationship we found between  $T_l$  and  $D_h$  had an average ratio  $T_l/D_h$  of about 100 (average 96.8, SD 26.2) which was in agreement with data reported by Jansen *et al.* (2011)

### *Pit anatomical characteristics*

Pit torus, chamber, and aperture areas followed a power trajectory with height in tree that paralleled the variation in tracheid diameters (Fig. 4 & 5), and these three traits had similar exponents of approximately 0.20. The classical study by Bailey and Faull (1934) on *Sequoia sempervirens* reporting positive correlations between pit size and tracheid dimensions on the one hand and tracheid size and trunk diameter and height on the other fully agrees with our findings. Our results are also congruent with some, but not all, more recent studies. Congruent with our observations, a decrease in aperture size with height in tree (Fig. 3) has been reported for Douglas-fir (Domec *et al.* 2006) and coast redwood (*Sequoia sempervirens*) (Burgess *et al.* 2006), and this trend was interpreted as a feature contributing substantial safety from runaway embolism at the expense of hydraulic conductance. In addition, Domec *et al.* (2008) reported for Douglas-fir that pit aperture decreased towards the tree top while torus diameter remained unchanged, resulting in an increase of the torus diameter/aperture diameter ratio that translates to a larger overlapping of the torus with the pit aperture. In giant sequoia we also found that aperture size decreased with height in tree, but torus area decreased concomitantly resulting in the ratio of torus/aperture areas very slightly decreasing (slope = 0.03 but significantly different from zero), not increasing, towards the tree top (Fig. 7). However, the torus overlap, calculated as proposed by Hacke and Jansen (2009), did not show any significant trend with tree height (data not shown), with values ranging from 0.16 to 0.82 (average 0.52).

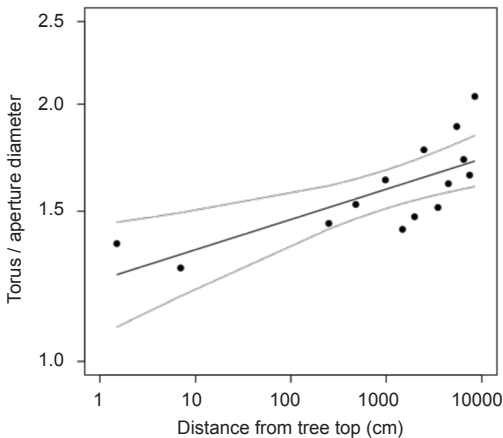


Figure 7. Variation in torus diameter/aperture diameter ratio vs distance from tree top ( $r^2 = 0.54$ ,  $p < 0.01$ ,  $b = 0.03$ ) in *Sequoiadendron giganteum*. The axes are shown in log-log scale. 95% confidence intervals are indicated by grey lines.

Recent findings (Schulte *et al.* 2015) showed that the structural properties of the margo change greatly within tree, with individual pores around the torus much wider, distance between pit borders larger, and margo membrane much thicker in wider tracheids. This collection of pit features likely affects the elastic properties of the membrane, including its deflection capacity.

Therefore, it is difficult to conclude that the structural features of the pits might induce a decrease in resistance to embolism towards the tree top, which reinforces the

idea that additional structural and functional measurements of pits are needed. In any case, the calculated torus/aperture size ratio values are within the same range of those reported by Domec *et al.* 2008 (*i.e.* between 1.2 and 2.0), suggesting that the observed trend was unlikely due to measurement errors.

The irregular variation in size of pit aperture along the stem (*e.g.* the maximum pit aperture was at about 50 m from the tree top) may be explained by the branching architecture of the selected giant sequoia tree. Indeed, the lowest living branches on this tree emerged from the trunk at ~40 m above the ground (Sillett *et al.* 2015), and the main trunk below this level may support a large number of old tree rings that are still active in the sapwood.

### ***Relative pit permeable area to lumen area is held constant***

We found that the total margo area occupied about 11.2%, (SD 1.96) of each tracheid cell wall independent of tracheid lumen area. This percentage is very similar to the 11.4% (SD 2.6) reported by Hacke and Jansen (2009), but higher compared to the 5.6% reported from Schulte (2012) in Douglas-fir and the 8.6% measured by Pittermann *et al.* (2006) in different conifer species. The area occupied by the margo should be related to the average margo permeability, thus future research could test the hypothesis that a lower proportion of margo area (*i.e.* 5%) is correlated to a higher amount of large pores which are the most important in determining the total permeability. Indeed, Schulte *et al.* (2015) demonstrated that the largest 25 pores out of 2500 account for about 40% of the total flow.

One important challenge in studying conduit hydraulic resistance is to disentangle the contribution of pit resistance to total hydraulic resistance (*i.e.*, pits plus lumina). Indeed as mentioned by Sperry *et al.* (2006) an increase in cell lumen size does not necessarily confer a decrease in resistance because water must also flow through the pits, and if pit resistance does not parallel the resistance imposed by variation in lumen diameter the decrease in total resistance might be lower than expected. Sperry *et al.* (2006) reported that the resistance of pits in conifers converges towards a constant fraction (64%) of the total tracheid resistance independently of species or tracheid diameter. This result elicits the hypothesis that, at least in conifers, anatomical traits important to water flow should vary in concert thus maintaining the pit resistance as a constant part of the whole conduit resistance.

According to this hypothesis, water transport would remain efficient with height growth and similar along the plant axis. Our data revealed that the total permeable area of the pits scaled isometrically with lumen area (Fig. 6) as already demonstrated in Douglas-fir (Schulte 2012). The total permeable area of pits was about 46 times the area of the lumen (*i.e.*, the value of the intercept). However, such isometric scaling would not be enough to completely compensate for the increase in flow due to a larger lumen area. Indeed, the flow scales with lumen area with an exponent of 2, thus the permeability of the margo membrane likely also scales with lumen area. Margo pore sizes were measured by Domec *et al.* (2006), who found their diameters to vary in parallel with torus and membrane diameters. Moreover, Schulte *et al.* (2015) found that margo pores were larger in roots compared to stems, suggesting that wider tracheids

also exhibit higher margo permeability. They also found that stems lumen resistance increased by of a factor of 6.7 and, in parallel, the total pit resistance increased by the same factor.

Collectively these results indicate that average size of margo pores scales isometrically with margo area, thus guaranteeing a more permeable area as pits increase in size and a parallel variation in potential flow between lumen area and pits. Our results suggest that along the stem axis multiple anatomical traits may be coordinated to stabilize the relative importance of pits vs lumen resistances, or, in other words suggested by Schulte *et al.* (2015), that a constant balance between the two components is maintained during tree growth.

These findings should be integrated into a model that predicts pit resistance to increase with tracheid diameter, thus limiting cell diameter (Lancashire & Ennos 2002). The assumptions of this model include 1) a constant pit number per tracheid, and 2) a constant density of pits, both of which were tested by our study. We found that pit number scaled isometrically with  $D_h$  (Fig. 5a), so pit number was not constant with  $D_h$ . We also found that pit density (*i.e.* number of pits per tracheid cell wall surface) is quite constant with  $L_t$  but, importantly, pit size (and in parallel the area of the individual pores of the membrane) decreased towards the tree top and, therefore, with  $D_h$ . The scaling relationships of the main anatomical properties demonstrated here might be useful for defining more realistic structures thus improving functional model predictions.

Our findings may also suggest a simple mechanism for determining the structure of the entire pipeline. The cambium can be considered programmed to produce a “standard” daughter cell with a given number of pits per unit of cell wall area. During the expansion phase tracheid diameter and pit dimensions change accordingly; if the expansion phase lasts longer (*i.e.* at the base) (Anfodillo *et al.* 2012), then tracheid diameter and pit traits (including average membrane pore area) should increase proportionally. These changes might simply be the consequence of a uniform cell wall expansion driven by turgor, similar to an “inflating balloon” on which the drawings at the surface enlarge proportionally with size. Thus, from a purely anatomical perspective the process driving the observed scaling relationships could be easily explained. This coordinated anatomical structure (*i.e.* pits and lumen in tandem) should be favoured by natural selection because both contribute to stabilizing the total resistance as trees grow taller. Although the physiological mechanisms controlling the duration of cell expansion along the stem axis await full clarification, a promising explanation is the longer duration of the expansion phase at the tree base due to a lower level of hormonal signal (*i.e.* auxin) delaying cell differentiation and maturation (Aloni & Zimmermann 1983).

## CONCLUSIONS

We analyzed axial variation in the tracheid anatomical features, including tracheid diameter and length as well as pit aperture, chamber, and torus areas, which are the most relevant to the transport of xylem sap through the main stem axis of a tall giant sequoia.

The traits varied in tandem suggesting a simple and stable anatomical organization that is maintained along the whole hydraulic pipeline. Our results show for this tall giant sequoia tree that: a) tracheids widen basipetally at a rate consistent with models positing that resistance can become independent of hydraulic path length; b) pit aperture, chamber, and torus areas are each correlated to variation in distance from tree top and therefore tracheid diameter, showing that a suite of axial anatomical adjustments occur in tandem with height in tree; c) the total permeable area of the margo is linearly related to the lumen area.

These results, in addition to the hypothesis that individual pores of the membrane should increase with size of pits, suggest that the resistance of pits scales isometrically with resistance of the lumen, which supports the notion that pits contribute a constant fraction of the total tracheid resistance. Our study provides new evidence that the hydraulic pathway is optimized for efficiency, thereby avoiding additional functional bottlenecks.

#### ACKNOWLEDGEMENTS

This study is part of a larger project examining axial conduit diameters in several species of tall trees (C. Williams *et al.* in prep.). The ideas investigated in this study were developed in the frame of the COST Action STReESS (FP1106). The authors thank the two anonymous reviewers for helpful comments and suggestions on an earlier version of the manuscript. We also thank personnel from Sequoia and Kings Canyon National Parks for permission to conduct scientific research. Alan Crivellaro was supported by the University of Padova (Assegno di Ricerca Junior (PDR124554/12)).

#### REFERENCES

- Aloni R & Zimmermann MH. 1983. The control of vessel size and density along the plant axis. *Differentiation* 24: 203–208.
- Anfodillo T, Carraro V, Carrer M, Fior C & Rossi S. 2006. Convergent tapering of xylem conduits in different woody species. *New Phytol.* 169: 279–290.
- Anfodillo T, Deslauriers A, Menardi R, Tedoldi L, Gai P & Rossi S. 2012. Widening of xylem conduits in a conifer tree depends on the longer time of cell expansion downwards along the stem. *Amer. J. Bot.* 63: 2117–2126.
- Anfodillo T, Petit G & Crivellaro A. 2013. Axial conduit widening in woody species: a still neglected anatomical pattern. *IAWA J.* 34: 352–364.
- Bailey IW & Faull AF. 1934. The cambium and its derivative tissues IX. Structural variability in the redwood *Sequoia sempervirens*, and its significance in the identification of fossil woods. *J. Arnold Arbor.* 15: 233–254.
- Becker P, Gribben RJ & Schulte PJ. 2003. Incorporation of transfer resistance between tracheary elements into hydraulic resistance models for tapered conduits. *Tree Physiology* 23: 1009–1019.
- Burgess SO, Pittermann J & Dawson TE. 2006. Hydraulic efficiency and safety of branch xylem increases with height in *Sequoia sempervirens* (D. Don) crowns. *Plant Cell Environ.* 29: 229–239.
- Choat B, Cobb AR & Jansen S. 2008. Structure and function of bordered pits: new discoveries and impacts on whole-plant hydraulic function. *New Phytol.* 177: 608–626.
- Comstock JP & Sperry JS. 2000. Theoretical considerations of optimal conduit length for water transport in vascular plants. *New Phytol.* 148: 195–218.

- Coomes DA, Jenkins KL & Cole LES. 2007. Scaling of tree vascular transport system along gradients of nutrient supply and altitude. *Biol. Lett.* 3: 86–89.
- Domec JC, Lachenbruch B & Meinzer FC. 2006. Bordered pits structure and function determine spatial patterns of air-seeding thresholds in xylem of Douglas-fir (*Pseudotsuga menziesii*; Pinaceae) trees. *Amer. J. Bot.* 93: 1588–1600.
- Domec JC, Lachenbruch B, Meinzer FC, Woodruff DR, Warren JM & McCulloh KA. 2008. Maximum height in a conifer is associated with conflicting requirements for xylem design. *PNAS* 105: 12069–12074.
- Gärtner H & Schweingruber FH. 2013. Microscopic preparation techniques for plant stem analysis. Kessel Publishing House, Remagen.
- Hacke UG & Jansen S. 2009. Embolism resistance of three boreal conifer species varies with pit structure. *New Phytol.* 182: 675–686.
- Jansen S, Lamy JB, Burlett R, Cochard H, Gasson P & Delzon S. 2011. Plasmodesmatal pores in the torus of bordered pit membranes affect cavitation resistance of conifer xylem. *Plant Cell Environ.* 35: 1109–1120.
- Lancashire JR & Ennos AR. 2002. Modelling the hydrodynamic resistance of bordered pits. *J. Exp. Bot.* 53: 1485–1493.
- Leicht MA. 2001. Vessel-element dimensions and frequency within the most current growth increment along the length of *Eucalyptus globulus* stems. *Trees* 15: 353–357.
- Li S, Lens F, Espino S, Karimi Z, Klepsch M, Schenk HJ, Schmitt M, Schuldt B & Jansen S. 2016. *IAWA J.* 37:152–171.
- McMahon TA & Kronauer RE. 1976. Tree structures: deducing the principle of mechanical design. *J. Theor. Biol.* 59: 443–436.
- Mencuccini M, Holtta MT, Petit G & Magnani F. 2007. Sanio's laws revisited. Size-dependent changes in the xylem architecture of trees. *Ecology Lett.* 10: 1084–1093.
- Olson EM, Anfodillo T, Rosell AJ, Petit G, Crivellaro A, Isnard S, Calixto LG, Alvarado-Cardenas LO & Castorena M. 2014. Universal hydraulics of the flowering plants: vessel diameter scales with stem length across angiosperm lineages, habits and climates. *Ecol. Lett.* 17: 988–997.
- Petit G & Anfodillo T. 2009. Plant physiology in theory and practice: an analysis of the WBE model for vascular plants. *J. Theor. Biol.* 259: 1–4.
- Petit G, Anfodillo T, Carraro V, Grani F & Carrer M. 2011. Hydraulic constraints limit height growth in trees at high altitude. *New Phytol.* 189: 241–252.
- Petit G, Anfodillo T & Mencuccini M. 2008. Tapering of xylem conduits and hydraulic limitations in sycamore (*Acer pseudoplatanus*) trees. *New Phytol.* 177: 653–664.
- Petit G, Pfausch S, Anfodillo T & Adams MA. 2010. The challenge of tree height in *Eucalyptus regnans*: when xylem tapering overcomes hydraulic resistance. *New Phytol.* 187: 1146–1153.
- Pittermann J, Sperry JS, Hacke UG, Wheeler JK & Sikkema EH. 2006. Inter-tracheid pitting and the hydraulic efficiency of conifer wood: the role of tracheid allometry and cavitation protection. *Amer. J. Bot.* 93: 1265–1273.
- Sanio K. 1872. Über die Grosse der Holzzellen bei der gemeinen Kiefer (*Pinus sylvestris*). *Jahrb. Wissen. Bot.* 8: 401–420.
- Schulte PJ. 2012. Vertical and radial profiles in tracheid characteristics along the trunk of Douglas-fir trees with implications for water transport. *Trees* 26: 421–433.
- Schulte PJ & Gibson AC. 1988. Hydraulic conductance and tracheid anatomy in six species of extant seed plants. *Can. J. Bot.* 66: 1073–1079.
- Schulte PJ, Hacke UG & Schoonmaker AL. 2015. Pit membrane structure is highly variable and accounts for a major resistance to water flow through tracheid pits in stems and roots of two boreal conifer species. *New Phytol.* 208: 102–113.

- Sillett SC, Van Pelt R, Carroll AL, Kramer RD, Ambrose AR & Trask D. 2015. How do tree structure and old age affect growth potential of California redwoods? *Ecol. Monogr.* 85: 181–212.
- Sperry JS, Hacke UG & Pittermann J. 2006. Size and function in conifer tracheids and angiosperm vessels. *Amer. J. Bot.* 93: 1490–1500.
- Sperry JS, Nichols KL, Sullivan JE & Eastlack M. 1994. Xylem embolism in ring porous, diffuse porous and coniferous trees of northern Utah and interior Alaska. *Ecology* 75: 1736–1752.
- Weitz JS, Ogle K & Horn HS. 2006. Ontogenetically stable hydraulic design in woody plants. *Funct. Ecol.* 20: 191–199.
- West GB, Brown JH & Enquist BJ. 1999. A general model for the structure and allometry of plant vascular systems. *Nature* 400: 664–667.

*Accepted: 15 February 2016*